



Soil loss estimation and susceptibility analysis using RUSLE and random forest algorithm: a case study of Nainital district, India

Yatendra Sharma¹ · Haroon Sajjad¹ · Tamal Kanti Saha¹ · Nirsobha Bhuyan¹ · Bharat Ratnu² · Geeta Kumari¹ · Raihan Ahmed³ · Daawar Bashir Ganaie¹

Received: 21 November 2024 / Revised: 22 March 2025 / Accepted: 24 March 2025
© The Author(s), under exclusive licence to Korea Spatial Information Society 2025

Abstract

The paper makes an attempt to estimate soil erosion and identify soil erosion susceptibility in Nainital district of India. The soil loss was estimated using Revised Universal Soil Loss Equation (RUSLE). Severe soil loss points extracted from the soil loss map and soil loss controlling factors were integrated to prepare soil erosion susceptibility map using random forest (RF) model. The effectiveness of the model was assessed using performance matrices. The soil loss and soil erosion susceptibility maps were validated using receivers operating characteristic (ROC) curve. The findings revealed that the largest area was under low soil loss class followed by moderate, high and very high classes. Steep slope, high rainfall erosivity, sparse vegetation and inadequate conservation practices have been identified for high and very high soil loss. The soil erosion susceptibility analysis through RF model revealed that nearly 35% area of the district is very highly susceptible due to deforestation, overgrazing and haphazard construction. The discussion with the communities during field work reaffirmed high soil loss and very high soil erosion susceptibility in northern part of the district. Integration of RUSLE and RF model may add a new dimension for devising effective soil conservation measures in spatial information science.

Keywords Soil loss · RUSLE model · Random forest · Nainital · Soil erosion susceptibility

✉ Haroon Sajjad
haroon.geog@gmail.com

Yatendra Sharma
syaten25@gmail.com

Tamal Kanti Saha
tamalkantisaha999@gmail.com

Nirsobha Bhuyan
nirsobhabhuyan08@gmail.com

Bharat Ratnu
bharatratnu2010@gmail.com

Geeta Kumari
gkyadav9111@gmail.com

Raihan Ahmed
raihan.nc2021@gmail.com

Daawar Bashir Ganaie
daawarb@gmail.com

¹ Department of Geography, Faculty of Natural Sciences, Jamia Millia Islamia, New Delhi, India

² Department of Geography, Shivaji College, University of Delhi, New Delhi, India

³ Department of Geography, Nowgong College, Nagaon, India

1 Introduction

Soil as a potential source of carbon sequestration can play a significant role in restricting global warming and mitigating climate change [1]. It helps in supply of nutrients to the vegetation and maintains its health [2]. The intensity of soil erosion has increased due to modification of interaction among soil, climate, landuse/ landcover, and topography [3]. Further, the increased frequency and intensity of precipitation and floods have caused the occurrence of soil erosion [4]. Water induced soil erosion is a major challenge of riverine countries across the world [5]. Soil erosion has caused reduction in crop productivity [6], deterioration of water quality [7], sedimentation and siltation of water bodies [8], and habitat destruction [9]. Climate change and anthropogenic activities induced soil loss have increased severe environmental implications [10].

Soil loss assessment and prediction using field based data is challenging and tedious task [11]. Integration of remote sensing techniques has helped in generating large volume of spatial data to assess soil erosion [12]. A large number of models have been developed for assessment and prediction

of soil loss at various scales such as [8], Universal Soil Loss Equation (USLE) model [13], Water Erosion Prediction Project [14], Revised Universal Soil Loss Equation (RUSLE) model [15], Unit Stream Power Based Erosion/ Deposition model (USPED) [16] and Hill Slope Model [17] are extensively used models for soil loss estimation. USLE and its improved version RUSLE models have been widely utilized for estimating soil loss [18]. More experiments, research and available resources have led to the development of the RUSLE model. Deterministic approach for calculating conservation practices (P) factor and minor changes in rainfall erosivity factor (R), crop management (C) factor, and slope length and steepness (LS) factor were incorporated in the revised model [19]. RUSLE model being empirical in nature has been given high consideration for estimating soil loss. It has an advantage over other models being capable of assessing pixel-based soil loss. While RUSLE aids in modelling the spatial patterns of soil erosion risk by considering environmental factors, its final erosion map often lacks accuracy. Moreover, RUSLE is constrained by the limited number of factors (R, K, LS, C, and P) for spatial erosion prediction. Machine learning algorithms are gaining popularity due to their demonstrated enhancements in accuracy, performance, and other notable strengths. Various models, including Boosted Regression Tree (BRT) [20], Random Forest (RF) [21], Naïve Bayes (NB) [22] and Artificial Neural Network (ANN) [23], are being widely used for soil loss assessment. The outcomes from all models demonstrated high accuracy and predictive capabilities. Mosavi et al. [24] have recently assessed soil erosion susceptibility employing the Weighted Subspace RF (WSRF), GaussprRadial, and NB models. Angileri et al. [25] utilized Stochastic Gradient Tree (SGT) based modelling to predict gully erosion. Svoray et al. [26] compared various data mining techniques, including SVM, Topographic Threshold (TT), ANN, Analytical Hierarchy Processes (AHP), and Decision Trees for modelling gully erosion susceptibility. These studies have demonstrated the effectiveness of machine learning models in soil erosion analysis.

The identification of soil loss susceptible hotspots is crucial in Nainital District, Uttarakhand, for several reasons, firstly, Nainital District is characterized by steep slopes and hilly terrain, making it highly susceptible to soil erosion. The region's topography accelerates the process of erosion, especially during heavy rainfall or snowmelt events. Secondly, soil erosion leads to the loss of fertile topsoil, which is essential for agriculture and vegetation growth. It also contributes to sedimentation in water bodies, such as lakes and rivers, affecting water quality and aquatic ecosystems. In district due to presence of many lakes, soil erosion can significantly impact the local environment. Thirdly, agriculture is a significant economic activity in Nainital District. Soil erosion can decrease crop productivity due to the loss

of nutrient-rich topsoil and land degradation. Fourthly, sedimentation in water bodies can affect hydropower generation and other water-dependent industries, impacting the local economy. Fifthly, soil erosion increases the risk of landslides, posing threats to infrastructure, human settlements, and lives. Nainital District has experienced several landslides in the past, often exacerbated by soil erosion, leading to loss of property and lives. The key objectives of the study were to estimate soil loss and identify soil erosion susceptibility. The study seeks to answer critical questions regarding the spatial distribution of soil loss, the effectiveness of RF in improving prediction accuracy of soil erosion susceptibility and devising effective soil conservation practices. Traditional empirical models namely USLE and RUSLE have been widely used for soil erosion assessment using predefined and limited parameters. The study introduces a novel approach by integrating RUSLE with the Random Forest (RF) machine learning algorithm for soil erosion susceptibility. The traditional RUSLE model relies on predefined factors such as rainfall erosivity, soil erodibility, slope length, crop management, and conservation practices that may not capture the complexity of site-specific conditions. The study utilized site-specific factors namely, elevation, slope, aspect, geology, geomorphology, land use/land cover, bare soil index, modified normalized difference water index, normalized difference vegetation index, and drainage density and employed RF for enhancing the predictive accuracy of soil erosion susceptibility mapping. The integration of RF allows for better handling of non-linear relationships and interactions among variables and providing a more nuanced understanding of soil erosion dynamics. This hybrid methodology has not only improved spatial prediction but also enabled the identification of high erosion susceptibility zones with greater precision. Thus, the data-driven framework involving traditional empirical RUSLE model with the RF machine learning algorithm may help in examining soil erosion susceptibility in different geographical regions and may be utilized as an effective methodology in spatial information science.

2 Materials and methods

2.1 Study area

Nainital district located in Uttarakhand state is a part of East Kumaon Himalaya in India. It is surrounded by Almora district in the north, Garhwal district in the north-west, Bijnor in the west, Udham Singh Nagar in the south and Champawat district in the east. The district spreads over a geographical area of 4251 sq km and stretches from 29°00'N to 29°05' N latitudes and from 78°80' E to 80°14' E longitudes (Fig. 1). The total population of Nainital district stands at

0.95 million, with a population density of 198 persons per square kilometre [27]. It is crisscrossed by numerous rivers and rivulets. *Kosi river* enter the district in the north near Khairana and flows in western direction Betalghat. The district comprises of three distinct geological regions namely Lower Himalayas, Shivalik and *Bhabhar*. Bhabhar covers the plains of the district and consists of recent alluvium. It is a narrow belt stretching along the foothills for eight to twenty-four kilometres in width. The hilly part of the district has several big and beautiful lakes such as Nainital, Bhimtal, Malwa Tal, Sat Tal, Naukuchhiya and Khurpa Tal. The soil

formation from various rock types like granite, schist, and limestone is influenced by the cool, moist climate [27]s. Steep hills and glacio-fluvial valleys primarily harbor shallow to moderately shallow, sandy-skeletal to loamy-skeletal soils, classified as Lithic/Typic Cryorthents, supporting sparse vegetation. The Lesser Himalayan range, rich in compressed rocks like granite and phyllites, is largely forested, with intermittent terraced cultivation on steep slopes. Deeper, well-drained soils with fine-loamy texture prevail in broader valley slopes, fostering wet and dry cultivation practices. The climate of the district varies depending on

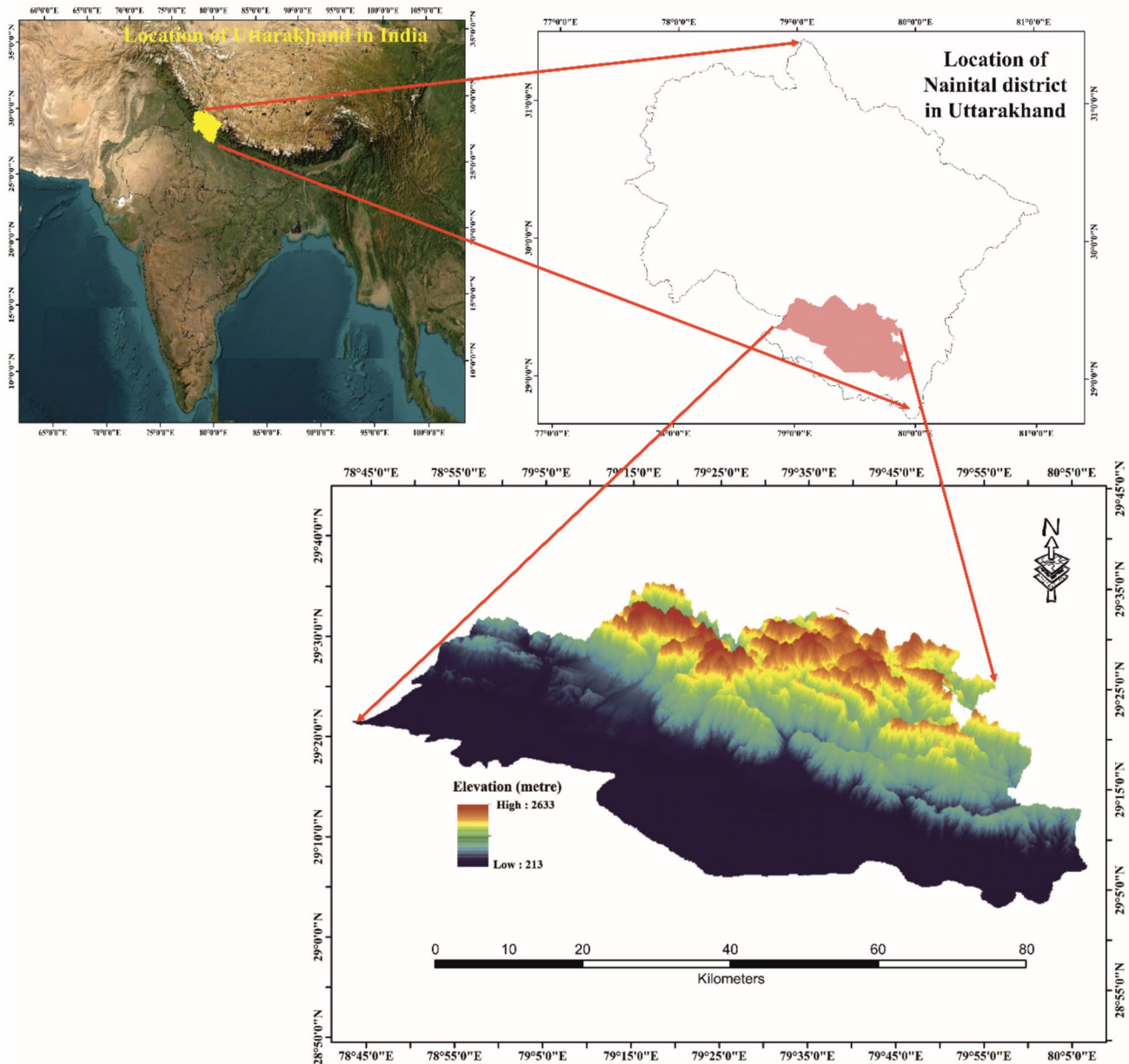


Fig. 1 Location of study area

the height. The study area experiences subtropical highland climate. The district receives an annual rainfall of 1300 mm and the maximum rainfall occurs in the month of June. Of the total geographical area of the district, the largest area (72%) is under forest. The main tree species in the study area includes *Populus ciliate*, *Quercus incana* Oak, *Fraxinus micrantha*, *Juglans regia*, *Aesculus indica*, etc. Steep hills and glaciofluvial valleys are dominated by acidic soil with low water-holding capacity.

In Nainital district, agriculture plays a vital role, engaging over 60% of the population. However, landholding sizes among farmers vary significantly, reflecting the diverse agricultural landscape. The hilly terrain and limited availability of flat land result in smaller average landholdings compared to plains regions. Typically, small and marginal farmers own plots of less than one hectare, while larger commercial operations may span several hectares. This variation is influenced by factors such as topography, land use patterns, and farming practices. Moreover, land fragmentation due to inheritance laws and population pressure further contributes to the diversity of landholding sizes in the district. The main crops cultivated in Nainital district vary according to the altitude, climate, and soil conditions. In the lower regions and valley areas, crops like rice, wheat, maize, and pulses are commonly grown. In the terraced fields on the hilly slopes, farmers cultivate crops such as millets, barley, and potatoes. Fruit orchards are also prevalent, with apples, peaches, pears, and plums being important cash crops. Additionally, vegetables like potatoes, tomatoes, peas, and leafy greens are grown for local consumption and market sale. Overall, the agricultural

diversity of Nainital district reflects its varied topography and microclimates.

2.2 Revised universal soil loss estimation

Cloud free pre-monsoon season Sentinel 2 satellite data (resolution 10m) for 2020 was downloaded from USGS Earth Explorer for assessing RUSLE. Survey of India topographical sheet on 1:50,000 scale was utilized for preparing the base map of the study area. Shuttle Radar Topography Mission (SRTM) digital elevation model (DEM) was downloaded from USGS Earth Explorer for generating the elevation map of the study area. Digital soil map of the world was downloaded from Food and Agricultural Organisation (FAO) Geo-network for preparing soil erodibility map. The point data of rainfall contained in 0.25 x 0.25° grid was downloaded from Indian Metrological Department (IMD). The details of the methodology are given in Fig. 2 and Table 1. RUSLE is a globally accepted and widely used empirical method of soil erosion estimation. It is a linear equation [18] (Eq. 1) and incorporates following five factors:

$$A = R * K * LS * C * P \quad (1)$$

where,

A = Average soil loss (tonnes/ha/year).

R = Rainfall erosivity factor (MJ mm/ha/h/year).

K = Soil erodibility factor (tonnes ha h/ha/MJ/mm).

LS = Slope length and steepness factor.

C = Cover and management practice factor.

P = Conservation practice factor.

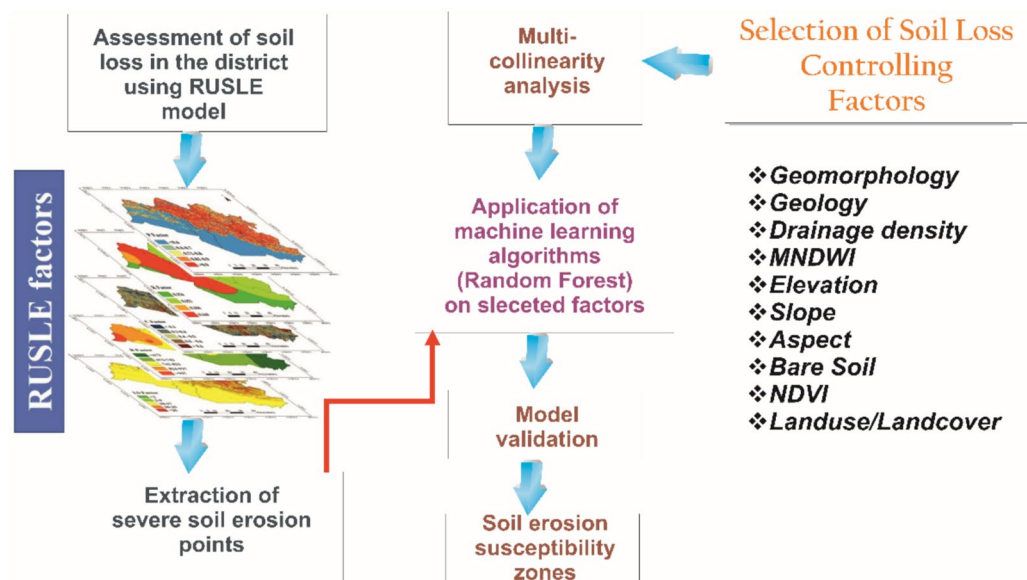


Fig. 2 Methodological framework for soil loss assessment and soil loss susceptibility mapping

Table 1 Sources of data

Data	Resolution	Year	Source
Sentinel 2	10 m	2020	USGS Earth Explorer
Topographical sheet	1:50,000	2005	Survey of India
SRTM DEM	30 m	2020	USGS Earth Explorer
Soil Map	1:5,000,000	1981	Food and Agricultural Organisation (FAO) Geo-network
Rainfall	0.25° × 0.25°	2020	India Metrological Department

2.2.1 R factor

R factor quantitatively represents the capacity of rainfall to transport and remove soil particles [28]. The erosivity is determined by the kinetic energy of the rainfall and greatly affected by the amount, intensity and duration of rainfall [11]. Average annual rainfall is directly proportional to R factor which can be used to estimate the R value [18]. R factor was determined by following Babu et al., [29] and (Eq. 2):

$$R = 22.8 + 0.6400 * MAP \quad (2)$$

where,

R = Rainfall Erosivity Factor (MJ mm/ha/h/year).

MAP = Mean Annual Precipitation (mm).

2.2.2 LS factor

LS factor is a combined factor of slope length and slope steepness. It shows the influence of landforms on soil erosion [30]. It depicts the impact of gravity on the flow and movement of water and hence it can help in examining the effect of landforms on soil loss [11]. Higher the value of LS factor, higher the rate of runoff and soil erosion. We determined LS factor following I. D. Moore and G. J. Burch, [31] equation was used (Eq. 3).

$$LS = (SlopeLength/22.13)^{0.4} \times (0.01745 \sin \theta / 0.0896)^{1.4} \times 1.4 \quad (3)$$

where,

Slope Length = Flow accumulation × Cell resolution (DEM).

θ = Slope in Degree.

2.2.3 C factor

Vegetation cover is also one of the influential factors for soil erosion estimation [32]. The C factor can be measured as the fraction of soil loss from vegetated areas to a continuously fallow land. C factor varies both temporally and spatially with respect to the relation between rainfall and vegetation cover.

Soil loss is inversely related with vegetation. The C factor was computed by using Normalized difference vegetation index (NDVI)[11]. NDVI quantifies vegetation health using reflectance differences between NIR (Near-Infrared) band and red band. The reflectance from the healthy vegetation increases dramatically in NIR band while the energy is absorbed in RED band due to presence of pigments in plant leaves.

and using Eq.4:

$$C = e^{[-2NDVI/(1-NDVI)]} \quad (4)$$

$$NDVI = \frac{NIR - Red}{NIR + Red} \quad (5)$$

where,

NDVI- Normalized Difference Vegetation Index.

NIR- Near Infrared Band.

RED- Red Band.

2.2.4 K factor

K factor indicates the soil sensitivity of soil to erosion. It also shows the transportation of sediment particles along with the runoff rate for a specified rainfall under a given condition. Soil erodibility has been assessed to know the possibility of soil loss for a particular type of soil. K factor denotes the soil holding capacity against transport processes as well as detachment. It is a function of permeability, structural integrity, antecedent moisture content, grain size, organic content, cohesiveness, porosity, parent material, texture and catena [11]. Digital soil map of the world obtained from Food and Agricultural Organization was utilized for assessing soil erodibility. K factor was computed by measuring the natural runoff (Eq.6):

$$K = 0.1317 * f_{Csand} * f_{CL-si} * f_{org} * f_{hisand} \quad (6)$$

where,

f_{Csand} = reduces K factor values for coarse textured sandy soils are low and increases for fine sandy soils; f_{CL-si} = lowers the value of k factor for high clay to silt fractions of a soil; f_{org} = reduces K values of the soil's rich in organic carbon, while f_{hisand} = reduces K value for the soils having high sand (Eq. 7–10):

$$f_{Csand} = \left\{ 0.2 + 0.3 \exp \left[-0.256 m_s \left(1 - \frac{m_{silt}}{100} \right) \right] \right\} \quad (7)$$

$$f_{CL-si} = \left(\frac{m_{silt}}{m_c + m_{silt}} \right)^{0.3} \quad (8)$$

$$f_{org} = \left\{ 1 - \frac{0.25 \text{ orgC}}{\text{orgC} + \exp[3.72 - 2.95 \text{ orgC}]} \right\} \quad (9)$$

$$f_{hisand} = 1 - \frac{0.7(1 - \frac{m_s}{100})}{1 - \frac{m_s}{100} + \exp[-5.51 + 22.9(1 - \frac{m_s}{100})]} \quad (10)$$

where, m_s is sand fraction content (%) having a diameter of 0.050–2.000 mm, m_{silt} is the silt fraction content (%) having diameter of 0.002–0.050 mm and m_c is clay fraction content (%) having diameter less than 0.002 mm and orgC is organic carbon content (%) [3].

2.2.5 P factor

P factor is the ratio between the conservation practice and the corresponding soil loss with downslope and upslope cultivation. The factor helps in examining the effects of tillage, contour farming and stone walls, etc. on soil loss. These practices help in reducing the amount of soil loss arising from high rainfall and consequent runoff rate [30]. P factor can be examined on the basis of field observation and visual image interpretation. The Eqn.11 developed by Wener, [33] was utilized for assessing the conservation practices. The equation describes the linkage between conservation practices and slope. The values range between 0 and 1, where 1 indicates no conservation practice was carried out and 0 indicates adoption of conservation practices. P factor can be numerically expressed as (Eq.11):

$$P = 0.2 + 0.03 \times S \quad (11)$$

where.

P = Conservation practice;

S = Slope (%).

2.3 Factors influencing soil erosion

Elevation serves as an important determinant of soil erosion, it influences microsite conditions that, in turn, impact plant distribution, morphology, physiology, and growth of plants [34]. The elevation data for the study area were obtained from the SRTM-DEM at a 30m spatial resolution, sourced from the USGS Earth Visualizing Viewer (Fig.3a). The slope is a critical topographical factor that significantly influences soil stability. It plays a pivotal role in determining the volume and velocity of runoff as well as sediment transport within a basin [35]. Steeper slopes are more prone to soil erosion compared to gentle slopes. The steeper slopes augment the channel's carrying capacity and elevate the risk of soil erosion [36]. The gradient of the district ranged from 17 to 92%, it was categorized into five classes: > 17%, 17–39%, 40–62%, 63–92%, and < 92% (Fig.3b). Drainage density, representing the total length of rivers, stands out as a crucial factor extensively utilized in modeling water-induced soil erosion. Drainage density serves as an indicator of resistance to both surface and deep soil erosion. Low

drainage density suggests high resistance, often associated with deep soil layers exhibiting high permeability and well-vegetated soil surfaces. Conversely, areas with impermeable deep soil layers and bare soil surfaces exhibit high drainage density, signifying rapid runoff discharge and an elevated risk of erosion [37]. The drainage density map depicts values ranging from 0.04 to over 2.34 km⁻¹ (Fig. 3c). Soil erosion processes are strongly influenced by types of land use. Generally, areas that are bare or sparsely vegetated tend to experience more rapid soil erosion. Five categories of landuse/landcover namely waterbody, open land, agriculture, built-up, and vegetation were identified in the study area (Fig. 3d). Large area of the district was found under vegetation. The majority of the Nainital district is characterized by vegetation.

The geography and climate of the Nainital district have produced the soils' varied properties. Steep hills and glacio-fluvial valleys are dominated by sandy-skeletal to loamy-skeletal soils, which have shallow depths, high drainage, and little water retention. Sparse vegetation is supported by these Lithic/Typic Cryorthents. On the other hand, fine-loamy soils with a fine texture, mild acidity, and a deeper, well-drained profile are found on the wider valley slopes (Fig. 4a). Modified normalized difference water index was used to assess the surface water. Riverbank erosion and accretion contribute to the pronounced spatial and temporal variability observed in the shapes and dimensions of rivers. A comprehensive understanding of the processes driving channel migration, erosion, and sediment deposition is crucial for effective management of soil loss. The values of MNDWI ranges from -0.46 to 0.22 (Fig. 4b). Vegetation cover serves as a protective factor against erosion [34]. Thus, the Normalized Difference Vegetation Index (NDVI) is a widely employed metric to characterize vegetation. The NDVI determined using near infrared (NIR) and red bands. NDVI is expressed as:

$$NDVI = \frac{NIR - RED}{NIR + RED} \quad (12)$$

The values of NDVI were classified into five classes namely <0, 0–0.2, 0.21–0.3, 0.31–0.5, and > 0.5 following Natural break method (Fig.4d).

The geological characteristics and rock types are crucial determinants influencing the erosion rate. The erodibility rate of the soil directly and indirectly impacts its compositional and structural characteristics [38]. The Nainital district lies in the lap of Himalyas in which the upper part is associated with certain geological features, while alluvium characterizes the middle to lower portions (Fig. 5a). This specific geological configuration is highly susceptible to erosion, with a substantial risk of large sediment volumes obstructing smooth water flow. This, in turn, has direct and indirect implications for decreasing the soil fertility of the

Fig. 3 Soil erosion influencing factors: a Elevation, b Slope, c Drainage density, and d Landuse/landcover

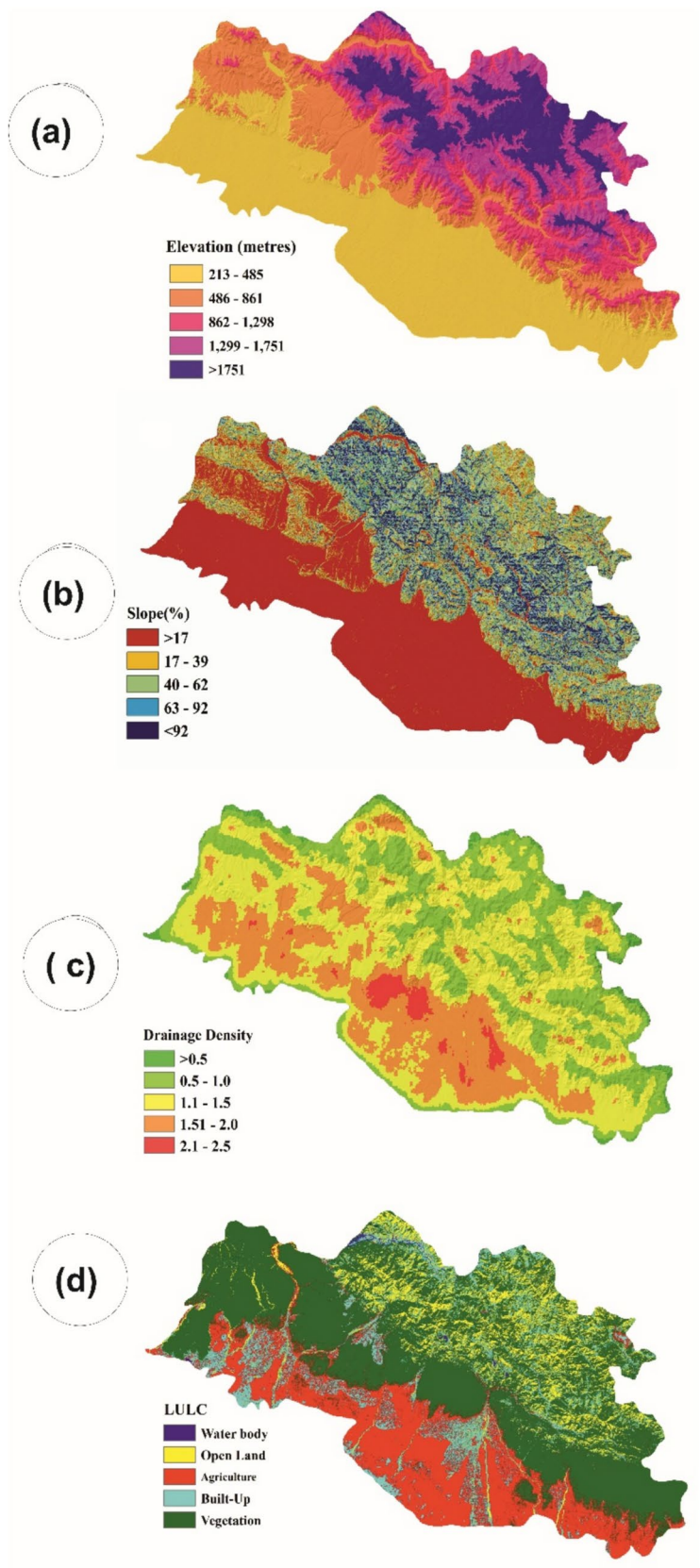


Fig. 4 Soil erosion influencing factors: a Soil, b MNDWI, c R Factor, and d NDVI

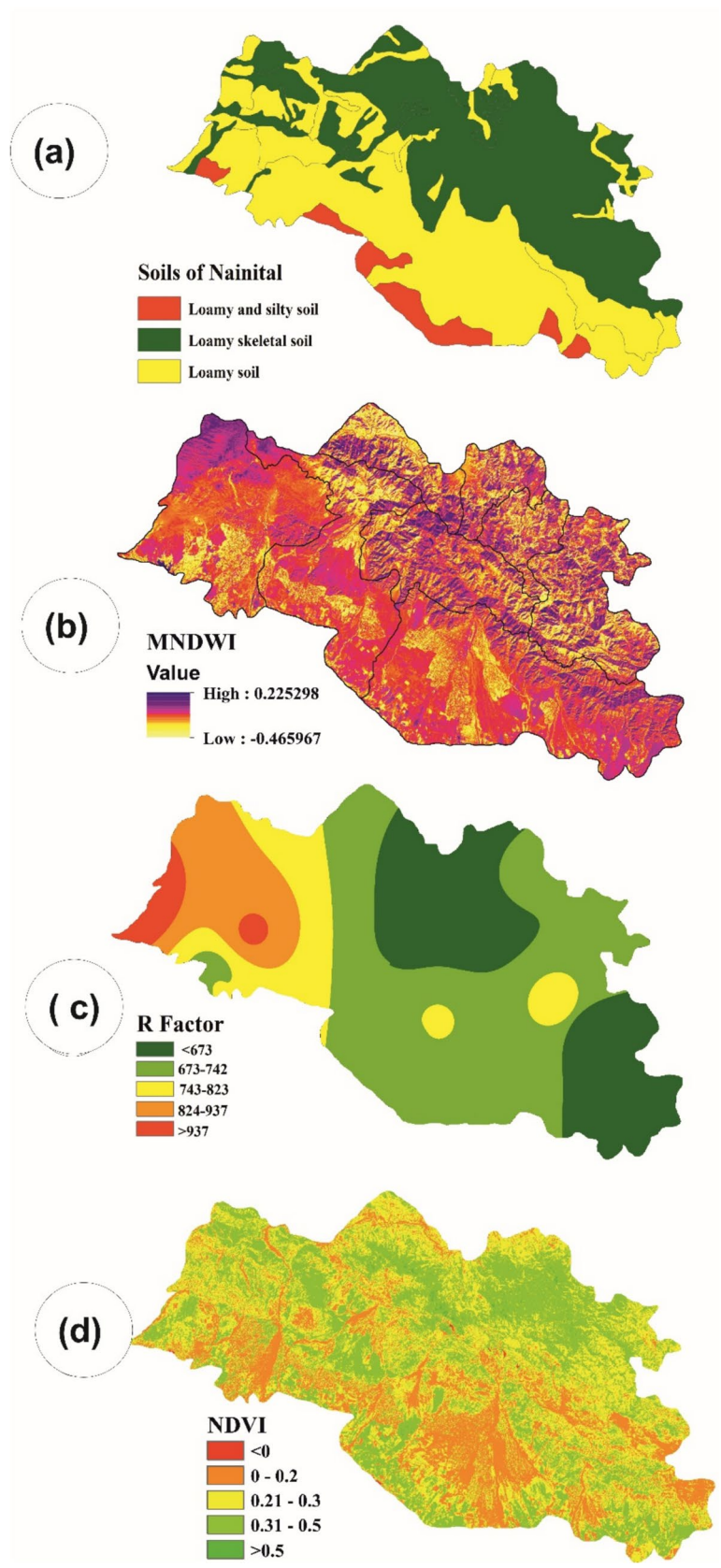
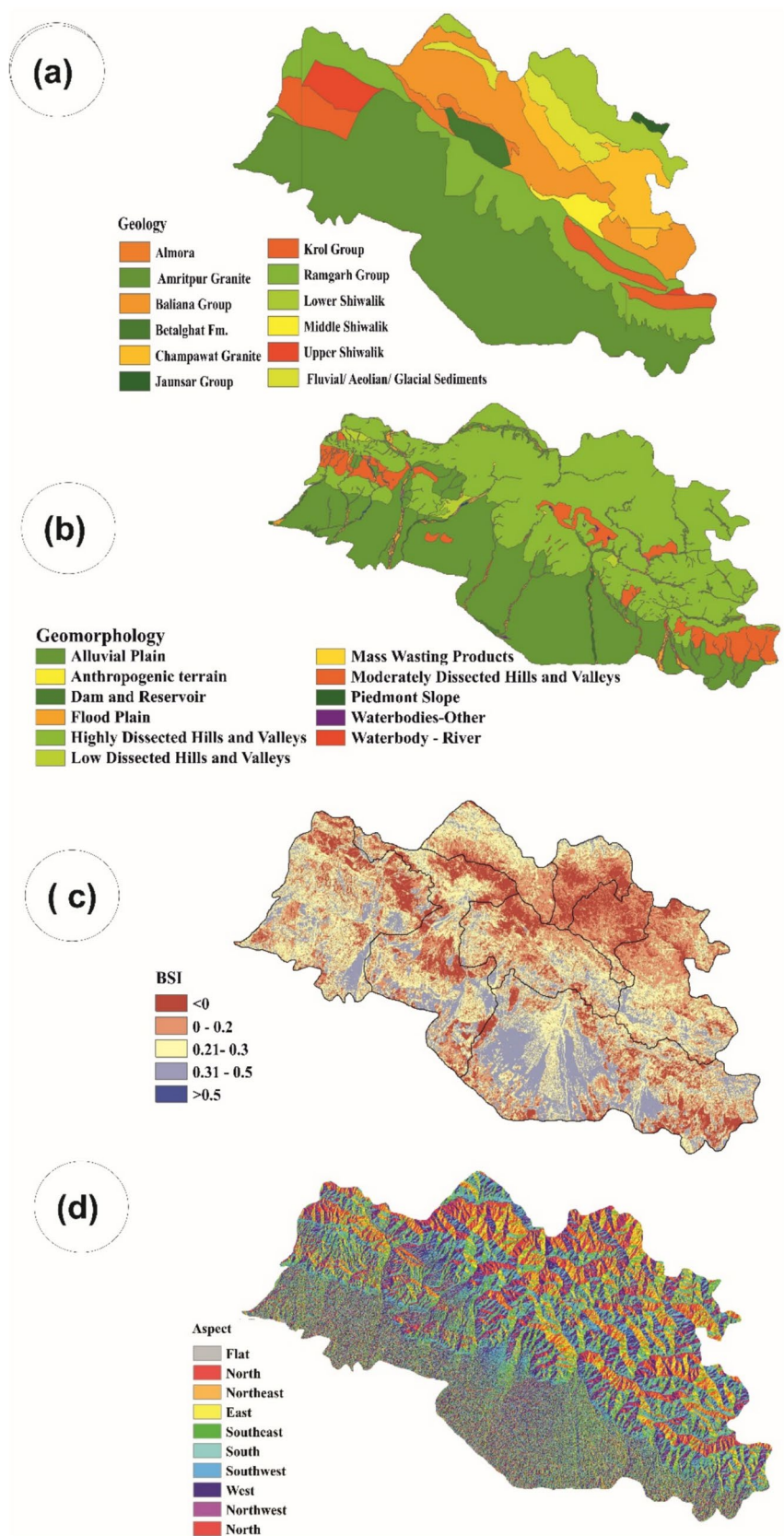


Fig. 5 Soil influencing factors:
 a Geology, b Geomorphology, c
 Bare soil d Aspect



lower and middle parts of the district. The diverse geological associations in the district plays varying roles in terms of erosion susceptibility. Geomorphology stands out as a paramount factor influencing susceptibility to soil erosion and rate of soil degradation through the formation and evolution of rills and gullies [39]. The upper section of the district is geographically situated in the foothills of Himalays (Fig. 5b). This particular morphological type, featuring steep slopes and the presence of rills and gullies, is deemed conducive to land degradation. Thus, geomorphological characteristics are considered as crucial determinant for soil susceptibility in sub-tropical regions. The bare soil index (BSI) discriminates area under vegetation and bare soil [34] (Fig. 5c). Surfaces exposed with little to no cover are highly susceptible to soil erosion, unlike covered ground that provides resistance against erosion. A low brightness index indicates the presence of vegetation cover while a higher brightness suggests barren land with soil or rock cover. In this study, the BSI was selected as one of the measures of soil susceptibility to erosion and was calculated as (Eq. 13):

$$BSI = \frac{(SWIR + RED) - (NIR + GREEN)}{(SWIR + RED) + (NIR + GREEN)} * 100 + 100 \quad (13)$$

Aspect plays a crucial role in regulating various climatic parameters, including sun and wind exposure (dry or wet conditions), precipitation intensity, and soil moisture [40]. The aspect map of the study area is depicted in Fig. 5d.

2.4 Multi-collinearity test

Accurate soil loss susceptibility mapping necessitates a meticulous consideration of site-specific soil loss controlling factors. To reduce interdependence among these factors, a multi-collinearity analysis was conducted by following [41]. This analysis addresses the situation where one inducing factor within a regression model can be accurately predicted. Both the Variance Inflation Factor (VIF) and Tolerance (TOL) methods were employed to assess the multicollinearity of the soil loss controlling factors. In a regression model, VIF and TOL serve as accepted measures to gauge the degree of multicollinearity of the n th independent variable with other variables. All selected factors were scrutinized for VIF and TOL to examine correlations among them. The application of the multi-collinearity test was crucial to minimize potential errors in the soil loss susceptibility mapping models. Equations 14 and 15 were utilized to calculate VIF and tolerances, respectively, in order to identify and address any issues related to multicollinearity.

$$Tolerance = 1 - r^2 \quad (14)$$

$$VIF = \frac{1}{Tolerance} \quad (15)$$

2.5 Random forest model

The Random Forest model, developed by Leo Breiman [42], is a robust machine learning algorithm for classification and regression. It builds an ensemble of decision trees trained on random subsets of data (bootstrapping) and features, reducing overfitting and enhancing diversity. This approach handles high-dimensional data, captures complex interactions, and is resilient to noise and outliers. Random Forest provides feature importance estimates and uses out-of-bag samples for internal validation, ensuring robust performance and aiding hyperparameter tuning.

2.6 Models validation

The performance of RUSLE model and was evaluated using ROC curve. These widely adopted metrics are instrumental in gauging model accuracy. Higher ROC values indicate a more effective model [34]. The area under the curve (AUC) in the ROC curve serves as a measure of goodness of fit and expresses the overall accuracy of the models. Typically, AUC values range between 0 and 1, where a value of 1 signifies a precise analytical test, and 0 denotes an inaccurate result. In constructing the ROC curve, sensitivity is plotted on the Y-axis, representing false positives, while specificity is plotted on the X-axis, reflecting false negatives. The accuracy of machine learning model was also assessed using AUC, accuracy, precision, recall, and F1-score, utilizing positive and negative sample sets by employing equations from 16 to 19.

$$Accuracy = \frac{TP + TN}{TP + TN + FP + FN} \quad (16)$$

$$Precision = \frac{TP}{TP + FP} \quad (17)$$

$$Recall = \frac{TP}{TP + FN} \quad (18)$$

$$F1Score = 2 * \frac{Precision * Recall}{Precision + Recall} \quad (19)$$

where,

TP= True Positive Pixel.

FP= False Positive Pixel.

FN= False Negative Pixel.

TN= True Negative Pixel.

3 Results

3.1 Soil loss estimation

Erosion is generally an outcome of rainfall events which causes more runoff and leads to detachment and transportation of soil particles. Higher chances of runoff from agricultural fields occur during spring season when the soil is saturated, snow is melted and vegetation cover is minimum [43]. The erosivity map was prepared through interpolation of rainfall data using inverse distance weighted method in GIS environment (Fig. 6a). The value of R factor varied between < 673 and > 937 MJ mm/ha/h/year. The rate of soil loss is determined by soil properties. Soils with high organic matter, high infiltration rate and better structure can help in restricting soil loss [43]. Soil erodibility (K factor) is an important factor of RUSLE model for estimating soil loss. The values of K factor ranged between 0.104 and 0.169 M J⁻¹ mm⁻¹. Higher values of this factor were observed in the

southern part of the district (Table 2&Fig. 6b). Soil loss is directly proportional to LS factor. It was derived using SRTM DEM slope map which, ranged between < 2 and > 25 (Fig. 6c). The findings revealed that the northern part of the district is highly vulnerable to soil loss. Thus, topography played an influencing role in regulating soil loss in the district. The values of C factor varied between 0.05 and 1. Lower values of C factor represented vegetation cover while higher values showed bare land. Lower values were mostly found in southern part of the study area. It is located at lower slope with large area under built-up and agricultural land (Fig. 6d). Higher values were observed in rocky area and bare land. This factor has contributed greatly to restrict soil loss in northern part. Though this area has high LS factor, but high vegetation covers restricted soil loss. The P factor helps in suggesting management practices for reducing soil loss [44]. Soil loss control practices were determined by using slope of the study area. Values of P Factor ranged from 0 to 1 where the values closed to 1 indicated weak management practices. P values were high in the northern part of

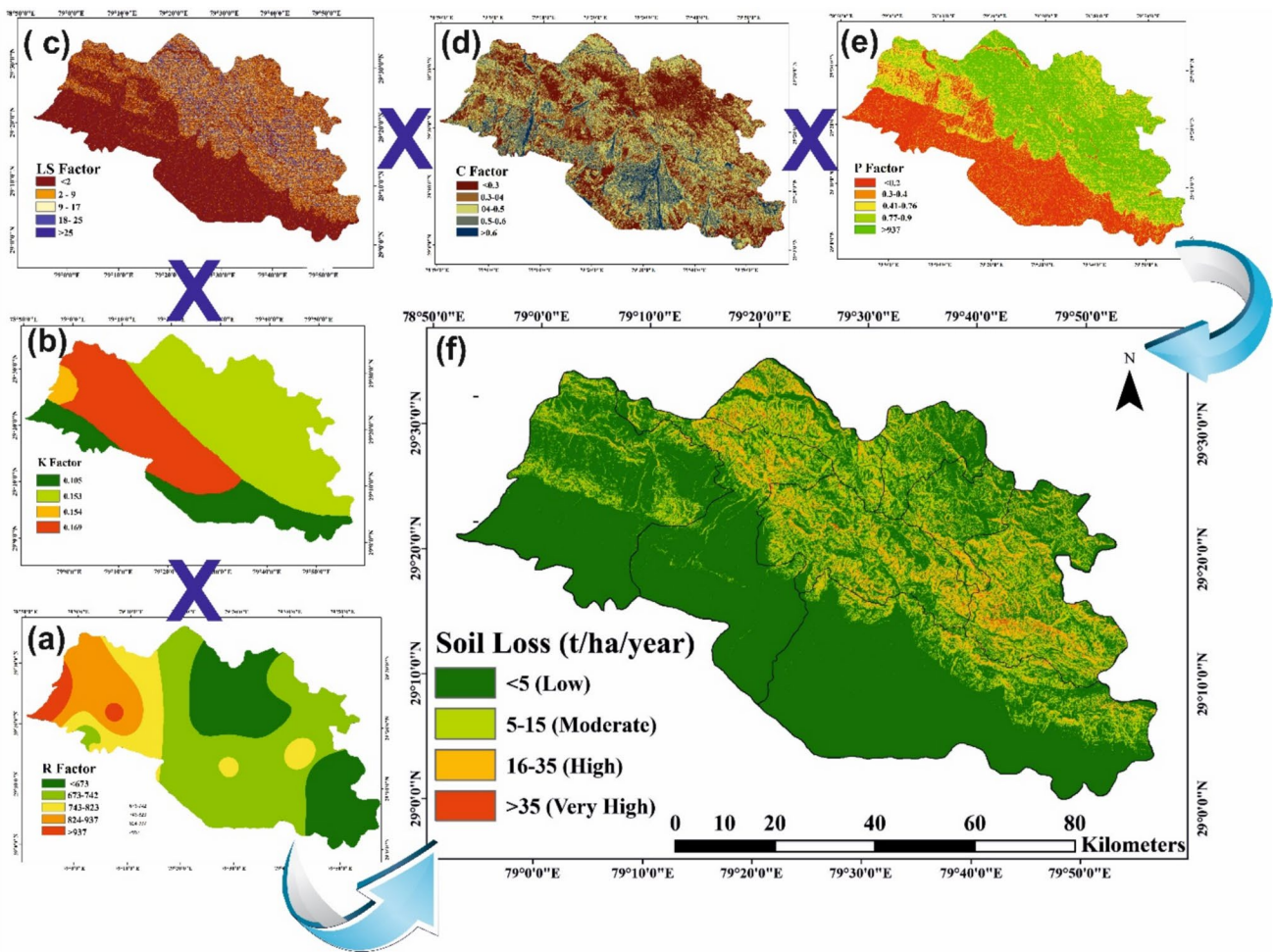


Fig. 6 Spatial pattern of a R factor, b K factor, c LS factor, d C factor, e P factor, and f Soil loss map derived using RUSLE

Table 2 Soil types and their K values

Soil Type	Sand %	Silt %	Clay %	Organic Carbon %	Area (%)	K value
Dystric Cambisols	32.7	30.3	37.1	3.28	50.51	0.153
Eutric Cambisols	36.4	37.2	26.4	1.07	30.08	0.169
Dystric Regosols	82.1	6.7	11.3	0.27	2.7	0.104
Eutric Gleysols	68.3	15.1	16.6	0.5	16.71	0.154

Table 3 Area under different soil loss classes. *Source* Authors' calculation from spatial analysis

Soil Loss (t/ha/year)	Area (%)
< 5 (Low)	69.79
5–15 (Moderate)	19.54
16–35 (High)	10.30
> 35 (Very High)	0.37

the district (Fig. 6e). Lack of soil management practices in this area has made this part highly vulnerable to soil loss.

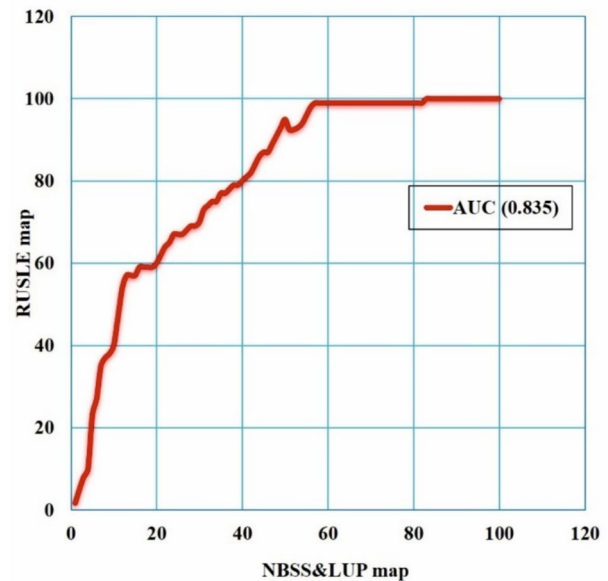
The P, K, LS, R and C factors were multiplied for generating soil loss map. Soil erosion values were classified into four soil erosion classes namely low, moderate, high, and very high soil loss using natural break method (Fig. 6f). The spatial distribution of soil loss has been shown in Fig. 6f. The table 3 revealed that largest area was under low soil loss (> 5 t/ha/year) followed by moderate (5–15 t/ha/year), high (16–35 t/ha/year) and very high (> 35 t/ha/year). Spatial distribution of soil loss in the district has revealed that northern part of the district experienced high and moderate soil loss. Larger area in southern part of the district was under low soil loss. This area is located in foothills of the study area and characterized with low soil erodibility, low length and steepness and large area under agriculture. The receiver operating characteristics (ROC) curve was used for validating the soil loss map. The area under curve (AUC) revealed 83% prediction rate (Fig. 7). Thus, RUSLE modelling approach has proved effective for soil loss estimation in Nainital district.

3.2 Multi-collinearity test

Interdependence among soil loss controlling parameters was examined through a multi-collinearity test. The presence of non-collinearity among factors was indicated by the Variance Inflation Factor (VIF) value exceeding 10 and the Tolerance (TOL) value being less than 0.1. Consequently, all the parameters were considered in the preparation of soil loss susceptibility map (Table 4).

3.3 Identification of soil loss susceptibility

The soil loss susceptibility mapping (Fig. 8) derived from RF model was classified into low (42.6%), moderate

**Fig. 7** ROC curve of the RUSLE model using the NBSS&LUP map for validation**Table 4** Analysis of collinearity between Soil loss controlling factors using the multicollinearity test

Soil loss controlling factors	Collinearity statistics	
	Tolerance	VIF
Elevation	0.248	4.030
Slope	0.294	3.406
Aspect	0.914	1.094
Bare soil	0.261	3.831
Geomorphology	0.223	4.479
Geology	0.427	2.342
Soil types	0.846	1.182
Landuse/Landcover	0.525	1.905
Drainage density	0.507	1.971
Rainfall erosivity factor	0.629	1.591
NDVI	0.259	3.856
MNDWI	0.683	1.463

(10.3%), high (12.4%) and very high (34.7%) soil loss susceptibility on the basis of Natural break method (Table 5). The soil loss susceptibility zones were identified by the RF model showed that the areas with very high susceptibility to soil loss are located in the north and north-eastern part of the district. In addition, the susceptibility map also showed that high to very high soil susceptibility zones are located in the areas which have high concentration of bare soil. The concentration of low to very low soil loss susceptibility zones were found mainly at the lower elevation and in the plain areas which are located in the southern part of the district.

3.4 Model validation

The model was validated using AUC, accuracy, precision, recall and F1 score. The higher the value of these assessors, better is the model's performance [34, 39]. The random forest model had a higher AUC value of 0.885 (Fig. 9). When the estimated AUC value is higher than 0.70, it indicates that the model's output and actual data are fairly aligned [40]. The Random Forest also performed better on the values of

Table 5 Area under different soil loss susceptibility zones

Soil loss susceptibility zones	RF	
	Area	% of area
Low	1811.19	42.60622
Moderate	437.115	10.28264
High	528.1291	12.42364
Very high	1474.566	34.6875

accuracy (0.889), precision (0.878), recall (0.898), and F1 score (0.888) (Table 6).

4 Discussion

This study utilized a novel approach by integrating the Revised Universal Soil Loss Equation (RUSLE), Geographic Information System (GIS) and Random Forest (RF) machine learning model for assessing soil erosion. The annual soil loss ranged between 0 and 150.70 t/ha/year. Kumar and Kushwaha, [45] also assessed soil loss

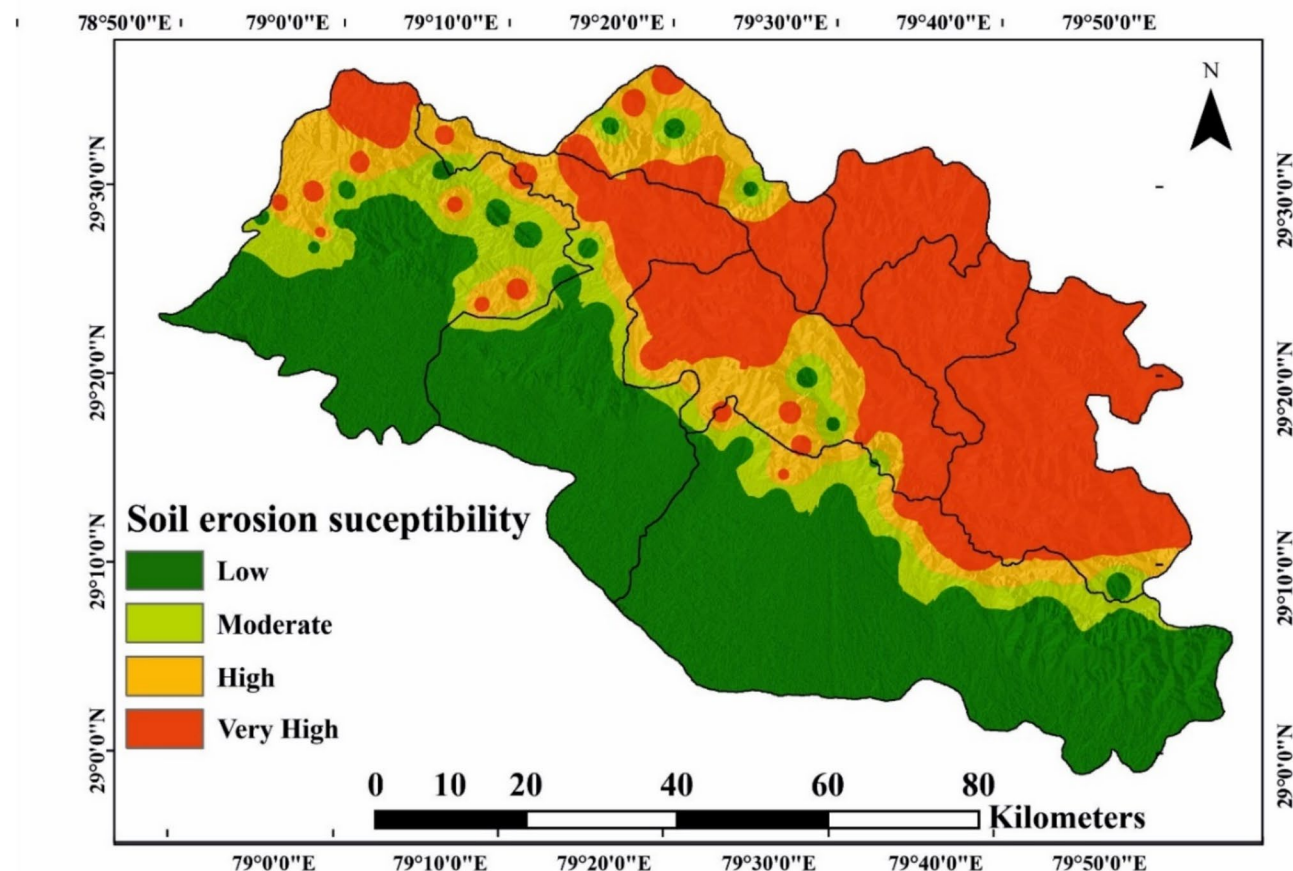


Fig. 8 Spatial distribution of soil loss susceptibility

Fig. 9 ROC curve for the soil erosion susceptibility zones model

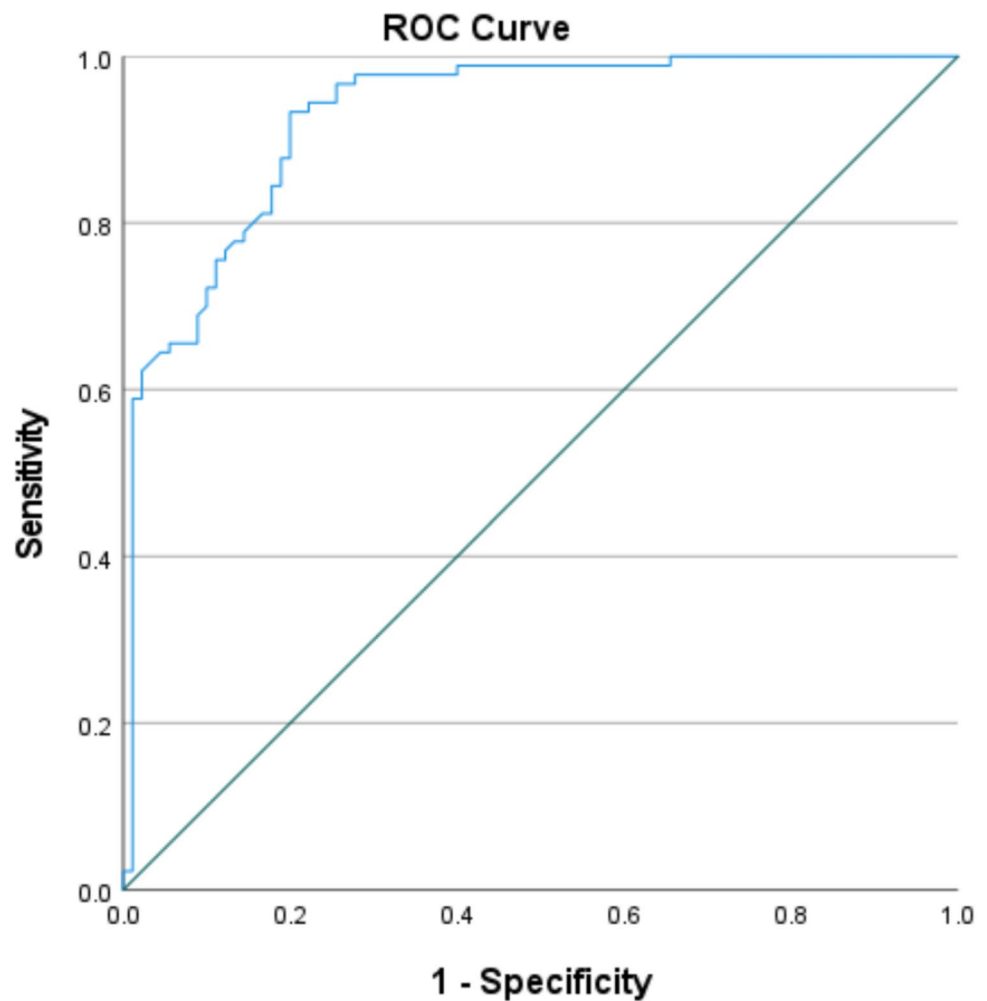


Table 6 Anomaly detection performance of random forest model

Metrics	Value
Accuracy	0.889
Precision	0.878
Recall	0.898
F1 Score	0.888
AUC	0.885

in Shiwalik sub watershed and found that the annual soil loss ranged between 8.50 and 138.9 t/ha/year. The northern part of the district experienced severe soil erosion. High elevation, steep slopes, and limited vegetation cover were identified as the influential drivers of soil erosion in this part. Similar results were reported by Bhandari and Wankhade [46] and Suthar et al. [47]. Strahler, (2020) [48] has emphasized the significant role of topography and slope gradient in accelerating erosion. Zhang et al. [49] and Fang et al. [50] who has identified steep slopes, increased run off velocity and reduced infiltration capacity as the major drivers of soil erosion due to increased

runoff velocity and reduced infiltration capacity. The areas with high drainage density experienced severe soil erosion. This finding is in line with study by Dragičević et al. [51] who has also highlighted the impact of drainage density on runoff and sediment transport. Low soil erosion was found in southern foothills mainly due to gentler slopes. Slope length and steepness in the northern part have caused greater runoff and erosion potential. The lower values of C-factor indicated higher vegetation cover. Thus, the denser vegetation in southern part has reduced soil loss. The higher values of P-factor indicated poor soil management practices. Further, deforestation, weak geological formation, occurrence of seismic events and increasing anthropogenic activities are attributed to higher soil loss in this part. The finding is in line with Mahapatra et al. [43]. The integration of RUSLE and RF models provided a robust method for estimating soil loss and identifying erosion hotspots. The RF model has shown its effectiveness in soil susceptibility mapping. Madarász et al. [52] and Tarek et al. [53] have also demonstrated the reliability of RF model in soil erosion analysis.

Severe land degradation has been observed due to soil erosion in the study area (Fig. 10). This is in with conformity of soil erosion susceptibility map. The haphazard construction of homes and hotels and the conversion of forest areas into agricultural land have increased soil erosion in the study area. Further, overgrazing has made topsoil susceptible to erosion. Thus, the study calls for targeted soil conservation measures, including a holistic approach blending engineering solutions, sustainable land management practices, and community participation. Afforestation and reforestation efforts are pivotal for stabilizing slopes, enhancing soil structure, and curbing surface runoff. Implementing terracing and contour farming techniques on hilly terrain can effectively reduce water flow velocity, trap sediment, and promote infiltration, thus preventing soil erosion. Adoption of soil conservation practices namely mulching, cover cropping, and crop rotation can help in improving soil health, increasing organic matter content, and shielding the soil surface from erosive forces. The construction of check dams and retention ponds along watercourses may help in regulating runoff, restricting sediment transport, and thwarting gully erosion. Establishment of vegetative barriers such as grass strips, hedges, and shrubs along slopes are suggested for stabilizing soil. Furthermore, implementing soil management techniques like minimum tillage, agroforestry, and alley cropping may help in enhancing soil structure, augmenting water infiltration, and reducing erosion risk. Public awareness campaigns are

essential for engaging local communities in soil conservation and long-term sustainability of conservation initiatives.

5 Conclusion

This study estimated the soil loss and identified soil erosion susceptibility in Nainital district of Uttarakhand, India. The soil loss was estimated using RUSLE. Site specific factors were utilized for analyzing soil erosion susceptibility using RF model. The soil loss map was validated using AUC-ROC curve. The effectiveness of RF model was examined using performance accessors. The findings revealed that the largest area of the district was found under low soil loss followed by moderate, high and very high. High and moderate soil loss was found in northern part of the district. Steep slopes, high drainage density and bare soil exposure have been attributed to high and moderate soil loss in this part. Soil erosion susceptibility analysis revealed that nearly 35% area of the district was found under high susceptibility. The findings emphasize the urgent need for targeted soil conservation measures, including afforestation, contour farming, and erosion control structures. Despite the effectiveness of hybrid modeling approach of RUSLE and RF in analyzing soil erosion, gully erosion and sediment transport could not be estimated. Long-term monitoring of soil erosion trends using high-resolution remote sensing data and assessment of

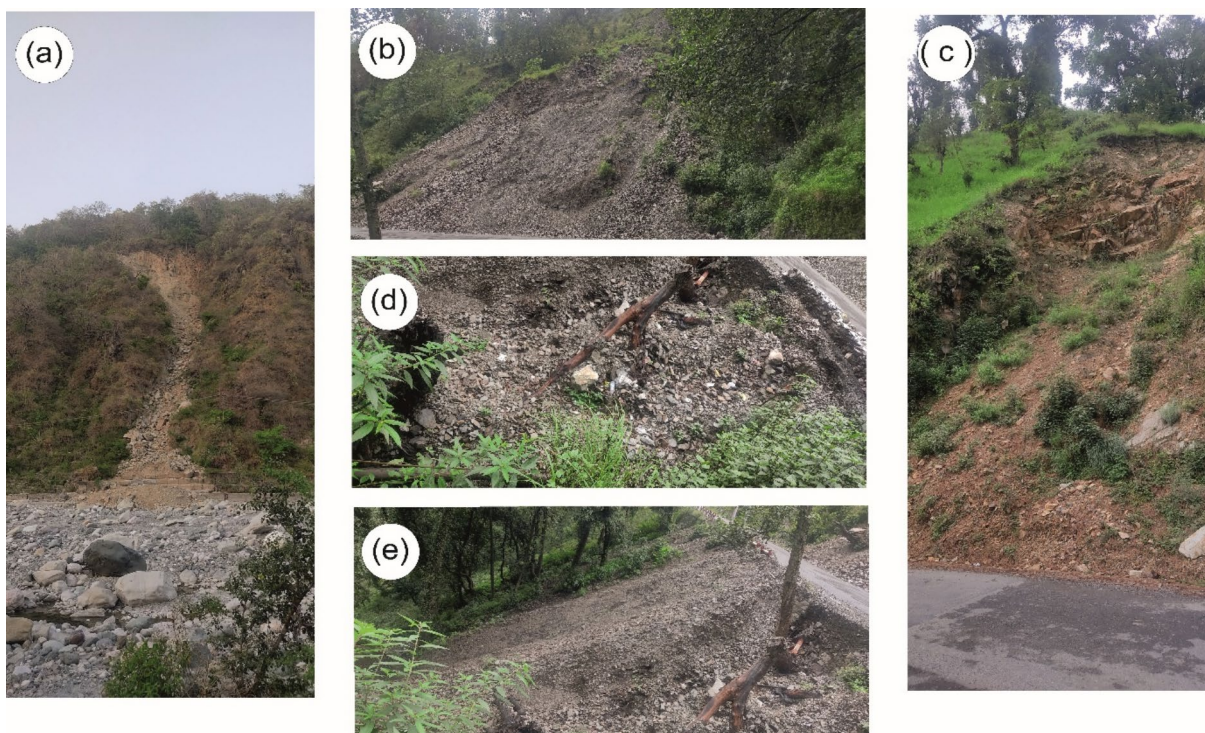


Fig. 10 Soil loss sites identified during field survey

the socio-economic impacts of soil loss need to be attempted in future research for devising effective soil conservation strategies.

Declarations

Conflict of interest The authors have no relevant financial or non-financial interests to disclose.

References

- Amelung, W., Bossio, D., de Vries, W., Kögel-Knabner, I., Lehmann, J., Amundson, R., Bol, R., Collins, C., Lal, R., Leifeld, J., et al. (2020). Towards a global-scale soil climate mitigation strategy. *Nature Communications*, *11*, 5427. <https://doi.org/10.1038/s41467-020-18887-7>
- Muledi, J., Bauman, D., Jacobs, A., Meerts, P., Shutcha, M., & Drouet, T. (2020). Tree growth, recruitment, and survival in a tropical dry woodland: The Importance of soil and functional identity of the neighbourhood. *Forest Ecology and Management*, *460*, 117894. <https://doi.org/10.1016/j.foreco.2020.117894>
- Pathan, S. A., & Sil, B. S. (2022). Prioritization of soil erosion prone areas in upper Brahmaputra river basin up to Majuli River Island. *Geocarto International*, *37*, 1999–2017. <https://doi.org/10.1080/10106049.2020.1810328>
- Li, X., & Wei, X. (2014). Analysis of the relationship between soil erosion risk and surplus floodwater during flood season. *Journal of Hydrologic Engineering*, *19*, 1294–1311. [https://doi.org/10.1061/\(ASCE\)HE.1943-5584.0000912](https://doi.org/10.1061/(ASCE)HE.1943-5584.0000912)
- Erci, V., Seker, C., Basaran, M., & Erpul, G. (2021). Determining the effectiveness of some soil stabilizers in wind erosion prevention using wind tunnel experiments. *Land Degradation Development*, *32*, 2962–2977. <https://doi.org/10.1002/ldr.3937>
- Lee, S., Chu, M. L., Guzman, J. A., & Botero-Acosta, A. (2021). A comprehensive modeling framework to evaluate soil erosion by water and tillage. *Journal of Environmental Management*, *279*, 111631. <https://doi.org/10.1016/j.jenvman.2020.111631>
- Ayele, H. S., & Atlabachew, M. (2021). Review of characterization, factors, impacts, and solutions of Lake Eutrophication: Lesson for Lake Tana Ethiopia. *Environmental Science and Pollution Res.*, *28*, 14233–14252. <https://doi.org/10.1007/s11356-020-12081-4>
- Das, B., Bordoloi, R., Thungon, L. T., Paul, A., Pandey, P. K., Mishra, M., & Tripathi, O. P. (2020). An integrated approach of GIS, RUSLE and AHP to model soil erosion in West Kameng watershed, Arunachal Pradesh. *Journal of Earth System Science*, *129*, 94. <https://doi.org/10.1007/s12040-020-1356-6>
- Chaudhry, S., Sidhu, G. P. S., & Paliwal, R. (2021). *Restoring ecosystem services of degraded forests in a changing climate* (pp. 353–375). Wiley.
- Negese, A., Fekadu, E., & Getnet, H. (2021). Potential soil loss estimation and erosion-prone area prioritization using RUSLE, GIS, and remote sensing in Chereti watershed, Northeastern Ethiopia. *Air, Soil Water Research*, *14*, 117862212098581. <https://doi.org/10.1177/1178622120985814>
- Meliho, M., Khattabi, A., & Mhammdi, N. (2020). Spatial assessment of soil erosion risk by integrating remote sensing and GIS techniques: A case of tensift watershed in Morocco. *Environment and Earth Science*, *79*, 207. <https://doi.org/10.1007/s12665-020-08955-y>
- Olorunfemi, I. E., Komolafe, A. A., Fasinmirin, J. T., Olufayo, A. A., & Akande, S. O. (2020). A GIS-based assessment of the potential soil erosion and flood hazard zones in Ekiti State, Southwestern Nigeria using integrated RUSLE and HAND Models. *CATENA*, *194*, 104725. <https://doi.org/10.1016/j.catena.2020.104725>
- Wischmeier, W.H., Smith, D.D. *Predicting Rainfall Erosion Losses--a Guide to Conservation Planning*; Agriculture; USDA, Washington, 1978.
- Flanagan, D. C., Nearing, M.A. USDA-water erosion prediction project (wepp) hillslope profile and watershed model documentation, nserl report #10. *Natl. Soil Eros. Res. West Lafayette*, *1995*, *10*, 1–123.
- Renard, K.G., Foster, G.R., Weesies, G.A., McCool, D.K., Yoder, D.C. *Predicting soil erosion by water : A guide to conservation planning with the revised universal soil loss equation (RUSLE).*; 1997.
- Mitas, L., & Mitasova, H. (1998). Distributed soil erosion simulation for effective erosion prevention. *Water Resources Research*, *34*, 505–516. <https://doi.org/10.1029/97WR03347>
- Grønsten, H. A., & Lundekvam, H. (2006). Prediction of surface runoff and soil loss in Southeastern Norway using the WEPP hillslope model. *Soil Tillage Research*, *85*, 186–199. <https://doi.org/10.1016/j.still.2005.01.008>
- Masroor, M., Sajjad, H., Rehman, S., Singh, R., Hibjur Rahaman, M., Sahana, M., Ahmed, R., & Avtar, R. (2022). Analysing the relationship between drought and soil erosion using vegetation health index and RUSLE models in Godavari middle sub-basin, India. *Geoscience Frontiers*, *13*, 101312. <https://doi.org/10.1016/j.gsf.2021.101312>
- Tiwari, A. K., Risse, L. M., & Nearing, M. A. (2000). Evaluation of WEPP and its comparison with USLE and RUSLE. *Transactions of the ASAE*, *43*, 1129–1135.
- Sahour, H., Gholami, V., Vazifedan, M., & Saeedi, S. (2021). Machine learning applications for water-induced soil erosion modeling and mapping. *Soil Tillage Research*, *211*, 105032. <https://doi.org/10.1016/j.still.2021.105032>
- Abedi, R., Costache, R., Shafizadeh-Moghadam, H., & Pham, Q. B. (2022). Flash-flood susceptibility mapping based on XGboost, random forest and boosted regression trees. *Geocarto International*, *37*, 5479–5496. <https://doi.org/10.1080/10106049.2021.1920636>
- Vu Dinh, T., Hoang, N.-D., & Tran, X.-L. (2021). Evaluation of different machine learning models for predicting soil erosion in tropical sloping lands of northeast Vietnam. *Applied and Environmental Soil Science*, *2021*, 1–14. <https://doi.org/10.1155/2021/6665485>
- Mehrabi, M., & Moayedi, H. (2021). Landslide susceptibility mapping using artificial neural network tuned by metaheuristic algorithms. *Environment and Earth Science*, *80*, 804. <https://doi.org/10.1007/s12665-021-10098-7>
- Mosavi, A., Sajedi-Hosseini, F., Choubin, B., Taromideh, F., Rahi, G., & Dineva, A. A. (2020). Susceptibility mapping of soil water erosion using machine learning models. *Water*, *12*(7), 1995. <https://doi.org/10.3390/w12071995>
- Angileri, S. E., Conoscenti, C., Hochschild, V., Märker, M., Rotigliano, E., & Agnesi, V. (2016). Water erosion susceptibility mapping by applying stochastic gradient treeboost to the Imera Meridionale river basin (Sicily, Italy). *Geomorphology*, *262*, 61–76. <https://doi.org/10.1016/j.geomorph.2016.03.018>

26. Svoray, T., Michailov, E., Cohen, A., Rokah, L., & Sturm, A. (2012). Predicting gully initiation: comparing data mining techniques, analytical hierarchy processes and the topographic threshold. *Earth Surface Processes and Landforms*, 37(6), 607–619. <https://doi.org/10.1002/esp.2273>
27. Sharma, Y., Sajjad, H., Saha, T. K., Bhuyan, N., Sharma, A., & Ahmed, R. (2024). Analyzing and forecasting climate variability in Nainital District, India using non-parametric methods and ensemble machine learning algorithms. *Theoretical and Applied Climatology*. <https://doi.org/10.1007/s00704-024-04920-y>
28. Xu, E., & Zhang, H. (2020). Change pathway and intersection of rainfall, soil, and land use influencing water-related soil erosion. *Ecological Indicators*, 113, 106281. <https://doi.org/10.1016/j.ecolind.2020.106281>
29. Babu, R.; Tejwani, K.; Agarwal, M.; Bhushan, L. Rainfall - intensity duration return period equations and nomographs of India. In Proceedings of the International conference on statistical climatology, Tokyo, Japan; Elsevier Scientific Publishing Co., 1979.
30. Polykretis, C., Alexakis, D. D., Grillakis, M. G., & Manoudakis, S. (2020). Assessment of intra-annual and inter-annual variabilities of soil erosion in Crete Island (Greece) by incorporating the dynamic “nature” of R and C-factors in RUSLE modeling. *Remote Sensing*, 12, 2439. <https://doi.org/10.3390/rs12152439>
31. Moore, I. D., & Burch, G. J. (1986). Modelling erosion and deposition: Topographic effects. *Transactions of the ASAE*, 29, 1624–1630. <https://doi.org/10.13031/2013.30363>
32. Ghosal, K., & Das Bhattacharya, S. (2020). A review of RUSLE model. *Journal of the Indian Society of Remote Sensing*, 48, 689–707. <https://doi.org/10.1007/s12524-019-01097-0>
33. Wener, C. *Soil Conservation in Kenya*. Nairobi; 1981
34. Sharma, Y., Ahmed, R., & Sajjad, H. (2022). Assessing vegetation condition across topography in Nainital District, India using temperature vegetation dryness index model. *Modeling Earth Systems and Environment*, 8, 2167–2181. <https://doi.org/10.1007/s40808-021-01208-2>
35. Zhang, P., Yao, W., Liu, G., Xiao, P., & Sun, W. (2020). Experimental study of sediment transport processes and size selectivity of eroded sediment on steep pisha sandstone slopes. *Geomorphology*, 363, 107211. <https://doi.org/10.1016/j.geomorph.2020.107211>
36. Arabameri, A., Tiefenbacher, J. P., Blaschke, T., Pradhan, B., & Tien Bui, D. (2020). Morphometric analysis for soil erosion susceptibility mapping using novel GIS-based ensemble model. *Remote Sensing*, 12, 874. <https://doi.org/10.3390/rs12050874>
37. Karmokar, S., & De, M. (2020). Flash flood risk assessment for drainage basins in the Himalayan foreland of Jalpaiguri and Darjeeling districts West Bengal. *Modeling Earth Systems and Environment*, 6, 2263–2289. <https://doi.org/10.1007/s40808-020-00807-9>
38. Chen, S., Zhang, G., Luo, Y., Zhou, H., Wang, K., & Wang, C. (2021). Soil erodibility indicators as affected by water level fluctuations in the three gorges reservoir area. *China. CATENA*, 207, 105692. <https://doi.org/10.1016/j.catena.2021.105692>
39. Bhuyan, N., Sajjad, H., Kanti Saha, T., Roshani, S., Sharma, Y., Masroor, M., Rahaman, M. H., & Ahmed, R. (2024). Assessing landscape ecological vulnerability to riverbank erosion in the middle Brahmaputra floodplains of Assam, India using machine learning algorithms. *CATENA*, 234, 107581. <https://doi.org/10.1016/j.catena.2023.107581>
40. Ahmed, R., & Sajjad, H. (2018). Analyzing factors of groundwater potential and its relation with population in the lower Barpani watershed, Assam, India. *Natural Resources Research*, 27, 503–515. <https://doi.org/10.1007/s11053-017-9367-y>
41. Sharma, Y., Ahmed, R., Saha, T. K., Bhuyan, N., Kumari, G., Roshani, Pal, S., & Sajjad, H. (2024). Assessment of groundwater potential and determination of influencing factors using remote sensing and machine learning algorithms: A study of Nainital District of Uttarakhand State, India. *Groundwater Sustain Development*, 25, 101094. <https://doi.org/10.1016/j.gsd.2024.101094>
42. Breiman, L. (2001). Random forests. *Machine Learn*, 45, 5–32. <https://doi.org/10.1023/A:1010933404324>
43. Mahapatra, S. K., Reddy, G. O., Nagdev, R., Yadav, R. P., Singh, S. K., & Sharda, V. N. (2018). Assessment of soil erosion in the fragile Himalayan ecosystem of Uttarakhand, India using USLE and GIS for sustainable productivity. *Current Science*, 115, 108–121.
44. Santra, A., & Santra Mitra, S. (2020). Space-time drought dynamics and soil erosion in Puruliya District of West Bengal, India: A conceptual design. *Journal Indian Society Remote Sensing*, 48, 1191–1205. <https://doi.org/10.1007/s12524-020-01147-y>
45. Kumar, S., & Kushwaha, S. P. S. (2013). Modelling soil erosion risk based on RUSLE-3D using GIS in a Shivalik sub-watershed. *Journal of Earth System Science*, 122, 389–398. <https://doi.org/10.1007/s12040-013-0276-0>
46. Bhandari, A., & Wankhade, H. (2025). Bivariate landslide susceptibility analysis for parts of Kumaon Himalayas: A case study of Nainital town and its surroundings, India. *Natural Hazards Research*. <https://doi.org/10.1016/j.nhres.2025.01.001>
47. Suthar, N., Das, D., & Mallik, J. (2024). Land-use suitability assessment for urban development using multi-criteria decision-making analysis in the Himalayan districts of Shimla, Nainital, and Darjeeling. *India. Discov. Environ.*, 2, 90. <https://doi.org/10.1007/s44274-024-00134-1>
48. Strahler, A. N. (2020). *The nature of induced erosion and aggradation* (pp. 18–35). Routledge.
49. Zhang, X., Hu, M., Guo, X., Yang, H., Zhang, Z., & Zhang, K. (2018). Effects of topographic factors on runoff and soil loss in southwest China. *CATENA*, 160, 394–402. <https://doi.org/10.1016/j.catena.2017.10.013>
50. Fang, H., Sun, L., & Tang, Z. (2015). Effects of rainfall and slope on runoff, soil erosion and rill development: An experimental study using two loess soils. *Hydrological Processes*, 29, 2649–2658. <https://doi.org/10.1002/hyp.10392>
51. Dragičević, N., Karleuša, B., & Ožanić, N. (2019). Different approaches to estimation of drainage density and their effect on the erosion potential method. *Water*, 11, 593. <https://doi.org/10.3390/w11030593>
52. Madarász, B., Jakab, G., Szalai, Z., Juhos, K., Kotroczó, Z., Tóth, A., & Ladányi, M. (2021). Long-term effects of conservation tillage on soil erosion in central Europe: A random forest-based approach. *Soil Tillage Research*, 209, 104959. <https://doi.org/10.1016/j.still.2021.104959>
53. Tarek, Z., Elshewey, A. M., Shohieb, S. M., Elhady, A. M., El-Attar, N. E., Elseoufi, S., & Shams, M. Y. (2023). Soil erosion status prediction using a novel random forest model optimized by random search method. *Sustainability*, 15, 7114. <https://doi.org/10.3390/su15097114>

Publisher's Note Springer Nature remains neutral with regard to jurisdictional claims in published maps and institutional affiliations.

Springer Nature or its licensor (e.g. a society or other partner) holds exclusive rights to this article under a publishing agreement with the author(s) or other rightsholder(s); author self-archiving of the accepted

manuscript version of this article is solely governed by the terms of such publishing agreement and applicable law.